

A bacterial-derived long chain fatty acid exhibits anti-inflammatory properties in colitis

Julien Pujo^{1,*,#}, Camille Petitfils^{1,*}, Pauline Le Faouder², Venessa Eeckhaut³, Gaëlle Payros¹, Sarah Maurel¹, Teresa Perez-Berezo¹, Matthias Van Hul⁴, Frédérick Barreau¹, Catherine Blanpied¹, Stéphane Chavanas⁵, Filip Van Immerseel³, Justine Bertrand-Michel², Eric Oswald^{1,6}, Claude Knauf^{1,7}, Gilles Dietrich¹, Patrice D. Cani^{4,7}, Nicolas Cenac^{1,&}

¹ IRSD, INSERM, INRA, INP-ENVT, Toulouse University 3 Paul Sabatier, Toulouse, France

² MetaToulLipidomics Facility, INSERM UMR1048, Toulouse, France

³ Department of Pathology, Bacteriology and Avian Diseases, Faculty of Veterinary Medicine, Ghent University, Merelbeke, Belgium

⁴ UCLouvain, Université catholique de Louvain, WELBIO- Walloon Excellence in Life Sciences and BIOTEchnology, Louvain Drug Research Institute, Metabolism and Nutrition Research Group, Brussels, Belgium.

⁵ Centre for Pathophysiology Toulouse-Purpan (CPTP), INSERM, CNRS, University of Toulouse, Toulouse, France.

⁶ CHU Toulouse, Hôpital Purpan, Service de bactériologie-hygiène, Toulouse, France

⁷ NeuroMicrobiota, European Associated Laboratory (EAL) INSERM/UCLouvain.

* Joint first author

current address: Farncombe Family Digestive Health Institute, McMaster University, Hamilton, Canada

Index

| | |
|-------------------------------|----|
| Supplementary methods..... | 2 |
| Supplementary results..... | 12 |
| Supplementary tables..... | 13 |
| Supplementary figures..... | 15 |
| Supplementary references..... | 30 |

Supplementary methods

Escherichia coli culture

One strain of *Escherichia coli* from the phylogenetic group A (MG1655) and eight strains from the phylogenetic group B2 including five pathogens (NC101, NU14, UTI, CFT, SP15), one asymptomatic (ABU), one commensal (M1/5) and one probiotic (EcN) were grown in agar LB plate for 12 to 18 hours at 37 °C (supplementary table 1). For each strain, a colony was grown in 3 mL of medium LB for 12 to 18 hours at 37 °C, then the volume corresponding to 0.1 unit of OD at 600 nm was seeded in 10 mL of Dulbecco's modified Eagle Medium (DMEM; Invitrogen, Cergy-Pontoise, France) containing 4.5 g/L of D-glucose, L-glutamine and 25 mM of HEPES during 8 hours before lipid extraction.

Holdemanella biformis culture

After growing *Holdemanella biformis* (DSM3989) for 72h in M2GSC broth (ATCC Medium: 2857) at 37°C in an anaerobic (80% N₂, 10% CO₂ and 10% H₂) workstation (GP-Campus, Jacomex, TCPS NV, Rotselaar, Belgium), the culture was streaked onto an agar plate containing M2GSC medium with 1,5% agar. After 48h incubation, DNA was extracted from the obtained colonies and PCR amplicons of the 16S rRNA gene were sent for Sanger sequencing to Eurofins Genomics Sequencing Europe (Konstanz, Germany) for confirmation of the species identity. Five broth cultures were grown for 72h; each culture was then diluted 1:25 into 10ml fresh M2GSC medium. After 48h of incubation at 37°C the cultures were centrifuged for 15min at 2319 x g at room temperature. Pellets and supernatant were stored at -20°C.

Extraction of bacterial lipids

Bacterial cultures were centrifuged at 755 g for 15 min and the recovered bacterial pellets were immediately crushed with a FastPrep-24 Instrument (MP Biomedical, Fisher scientific SAS, Illkirch, France) in 200 μ L HBSS (Invitrogen) and 5 μ L internal standard (IS) mixture (Deuterium-labeled compounds) (400 ng mL⁻¹). After two crush cycles (6.5 ms⁻¹, 30 s), 10 μ L of suspensions were withdrawn for protein quantification and 0.3 mL of cold methanol (MeOH) were added. In parallel, bacteria culture supernatants were filtered through a 0.22- μ m pore size filter (Merck Chimie SAS, Fontenay Sous Bois, France) to remove residual bacterial cells, and 1 mL of supernatant was collected for lipid extraction after addition of 5 μ L IS mixture and 0.3 mL of cold MeOH. Both bacteria and supernatant samples were centrifuged at 1016 \times g for 15 min (4 °C) and the resulting supernatants were submitted to solid phase extraction of lipids using HLB plate (OASIS® HLB mg, 96-well plate, Waters, Saint-Quentin-en-Yvelines, France). Briefly, plates were conditioned with 500 μ L MeOH and 500 μ L H₂O/MeOH (90:10, v/v). Samples were loaded at a flow rate of about one drop per 2 s and, after complete loading, columns were washed with 500 μ L H₂O/MeOH (90:10, v/v). The columns were thereafter dried under aspiration and lipids were eluted with 750 μ L MeOH. Solvent was evaporated under N₂ and samples were resuspended with 140 μ L MeOH and transferred into a vial (Macherey-Nagel, Hoerd, France). Finally, the 140 μ L of methanol were evaporated and our sample resuspended with 10 μ L of methanol for liquid chromatography/mass spectrometry analysis

Identification of hydroxylated long chain fatty acid

MS and MS/MS analyses were performed in the negative ion FTMS mode at a resolution of 30,000 (at m/z 400) with the following source parameters: capillary temperature was 325 °C, source heater temperature was 300 °C, sheath gas flow rate was 30 a.u. (arbitrary unit), auxiliary gas flow rate was 10 (a.u.), and source voltage was -2.9 kV. Samples were injected on a ZorBAX SB 120 C18 column (2.1 \times 100 mm, 2.7 μ m) (Agilent Technologies) maintained at 40 °C. Solvent A was 0.1% formic acid in H₂O and solvent B was 0.1% formic acid in

acetonitrile at a flow rate of 350 $\mu\text{L min}^{-1}$. The multistep gradient was as follows: 25% B at 0 min, 40% B at 10 min, 47.5% B at 10.1 min, 73.8% B at 21 min, 100% B at 21.2 min, 100% B at 23.2 min, 25% B at 23.4 min, and 25% B at 25.4 min. The autosampler was set at 5 °C and the injection volume was 5 μL . The identification and the data processing were performed using XCalibur software (Thermo Fisher Scientific). The MS/MS experiments were performed by using collisional activation within non-resonant excitation mode (HCD32). The excitation energy was optimized in the range of the 20 and 35% NCE such as the precursor ion survived to the dissociation processes within a relative abundance between 30 and 150% of the most abundant product ion displayed in the HCD spectrum recorded with a resolution of 30,000.

Quantification of hydroxylated long chain fatty acid

In bacteria, we quantified C8-3OH, 12-TriHOME, 10-TriHOME, C10-3OH, C12-3OH, 12,13-DiHOME, 9,10-DiHOME, 9-HOTrE, 13-HOTrE, 13-HODE, 9-HODE, C14-3OH, 13-OxoODE, 9-Oxo-ODE, C16:1-3OH, C16-3OH, C18:1-3OH and C18-3OH (supplementary Table 2). All the standards were purchased from Avanti® Polar Lipids (Merck – Sigma Aldrich, St. Quentin Fallavier, France). The quantification of hydroxylated long chain fatty acid was performed on a high-performance liquid chromatography (Agilent 1290 Infinity) coupled to a triple quadrupole mass spectrometer (G6460 Agilent). Samples were injected on a ZorBAX SB 120 C18 column (2.1 \times 100 mm, 2.7 μm) (Agilent Technologies) maintained at 40 °C. Solvent A was 0.1% formic acid in H₂O and solvent B was 0.1% formic acid in acetonitrile at a flow rate of 350 $\mu\text{L min}^{-1}$. The linear gradient was as follows: 30% B at 0 min, 85% B at 15 min, 100% B at 15.1 min, 100% B at 16.5 min, and 30% B at 16.7 min. The autosampler was set at 5 °C and the injection volume was 5 μL . The HPLC system was coupled online to an Agilent 6460 triple quadrupole MS (Agilent Technologies) equipped with an ESI source. ESI was performed in negative ion mode. Source parameters used were as follows: source temperature was set at 325 °C, nebulizer gas (nitrogen) flow rate was 10 L min⁻¹, sheath gas temperature

was 400 °C, sheath gas (nitrogen) flow rate was 12 L min⁻¹, and the spray voltage was adjusted to -3.5 kV. Analyses were performed in Selected Reaction Monitoring detection mode (SRM) using nitrogen as collision gas. Ion optics and collision energy were optimized for each hydroxylated fatty acid (supplementary table 2). In order to increase the sensibility, the mass method was segmented and the dwell times were optimized for each segment. Finally, peak detection, integration and quantitative analysis were done using MassHunter Quantitative analysis software (Agilent Technologies).

Colitis induction and study design

For all *in vivo* colitis studies, 4 groups of 5 mice were used per experiment and replicated 3 times. Dextran sulfate sodium (DSS; molecular weight, 40 kDa; MP Biomedicals, Fisher Scientific, Illkirch, France) colitis was induced in C57Bl/6J mice that, for 7 days, received 3% DSS dissolved in their drinking water. No mortality was observed during the 7 days of DSS administration in all groups. Development of colitis was assessed daily by measurement of the body weight. Paracellular permeability, macroscopic and microscopic damage score were evaluated after 7 days of DSS. Colonic tissue samples were also harvested to perform RT-qPCR and polyunsaturated fatty acid (PUFA) metabolites quantification.

In a first set of experiments, mice were gavaged every day for 9 days (2 days before and during the 7 days of DSS treatment) with 100 µM of C18-3OH (Avanti® Polar Lipids, Merck – Sigma Aldrich) solubilized in 100 µL of PBS/ethanol 3% or with the vehicle (PBS/ethanol 3%). In a second series of experiment, mice received fructooligosaccharides (10%, FOS; Beneo-Orafti, Oreye, France) in the drinking water for 10 days (3 days before and during the 7 days of DSS treatment). For these second series of experiment, abundance of bacteria genera in caecal microbiota was determined.

Paracellular permeability, macroscopic and microscopic score assessment

To determine paracellular permeability, at the end of the DSS-treatment, mice were gavaged with dextran 4kDa-FITC (25 mM; Sigma, St. Quentin Fallavier, France). Four hours after, mice were sacrificed blood was collected for FITC quantification in the serum and the colons were removed. Length and thickness were measured and macroscopic colonic tissue damages were scored from 0 to 3 for the intensity of adhesion and strictures, from 0 to 2 for the intensity of oedema, erythema, ulceration and diarrhoea and from 0 to 1 (absent or present) for the mucus, haemorrhage and faecal blood; the maximal score being 17. For histological examination, a specimen of colon located at 2 cm proximal to the anus was resected, fixed in 10% phosphate-buffered formalin, embedded in paraffin, sectioned, and stained with hematoxylin–eosin. Slides were examined and graded for cellular infiltration, mucosal architecture alteration and submucosal oedema from 0 to 3 (absent, mild, moderate and severe) and vasculitis, muscular thickening, crypt abscess and goblet cell depletion from 0 to 1 (absent or present); the maximal score being 13.

Real time PCR analysis

Colon biopsies were crushed in 500 mL of Trizol (Molecular Research Center, Euromedex, Souffelweyersheim, France) in Precellys lysing kit tubes (Bertin Technologies, Montigny le Bretonneux, France) placed in a Precellys (2823g, 30 seconds twice; Bertin Technologies). After addition of chloroform and centrifugation (15 minutes, 1019 g at 4°C), the supernatant containing the RNA was removed. Ethanol 70% (vol/vol) was added and the contents were placed in columns (GenElute® mammalian total RNA miniprep kit, Sigma Aldrich). The RNA was extracted according to the manufacturer recommendations. Subsequently the RNA were dosed in a nanodrop (implenGmbH, Dominique Dutscher, Issy-les-Moulineaux, France). RNA (10 µg) preparations from colon of DSS mice were purified using the kit (Dynabeads® mRNA purification kit, Fisher Scientific, Illkirch France) according to the manufacturer recommendations. Then, total RNA was reverse-transcribed with Moloney murine leukemia

virus reverse transcriptase (Fisher Scientific) using random hexamers (Fisher Scientific) for priming. Transcripts encoding hypoxanthine phosphoribosyl transferase (*Hprt*), trefoil factor 3 (*Tff3*), *mucin 2* (*Muc2*), occludin, zonula occludens-1 (*Tjp1*), regenerating islet-derived 3 gamma (*Reg3γ*), matrilysin (*Mmp7*), tumor necrosis factor alpha (*Tnfα*), chemokine (C-C motif) ligand 5 (*Ccl5*), transforming growth factor beta (*Tgfβ*), interleukin 6 (*Il6*), *Il1β*, nuclear factor kappa B (*Nfkb*), chemokine (C-X-C motif) 1 ligand (*Cxcl1*), *Cxcl2*, fasting-inducing adipocyte factor (*Fiaf*) and liver-fatty acid binding protein (*Lfabp*) were quantified by real-time PCR using specific forward and reverse primers (supplementary table 3), the kit Takyon No ROX SYBR 2X MasterMix blue dTTP (Eurogentec) and the LightCycler480II (Roche Diagnostics, Meylan, France).

PUFA metabolites LC-MS/MS measurements

PUFA metabolites were extracted following the methods previously described for bacterial lipids. 6-keto-prostaglandin F1 alpha (6kPGF_{1α}), thromboxane B2 (TxB₂), PGE₂, 8-isoPGA₂, PGE₃, 15d-PGJ₂, PGD₂, lipoxin A4 (LxA₄), LxB₄, resolvin D1 (RvD1), RvD2, RvD5, 7-Maresin 1 (7-Mar1), leukotriene B₄ (LtB₄), LtB₅, protectin Dx (PDx), 18-hydroxyeicosapentaenoic (18-HEPE), 5,6-dihydroxyeicosatetraenoic acid (5,6-DiHETE), 9-hydroxyoctadecadienoic acid (9-HODE), 13-HODE, 15-hydroxyeicosatetraenoic acid (15-HETE), 12-HETE, 8-HETE, 5-HETE, 17-hydroxydocosaheptaenoic acid (17-HDoHE), 14-HDoHE, 14,15-epoxyeicosatrienoic acid (14,15-EET), 11,12-EET, 8,9-EET, 5,6-EET, and 5-oxoeicosatetraenoic acid (5-oxoETE) were quantified in mouse colons.[1] To simultaneously separate 31 lipids of interest and three deuterated internal standards (5-HETEd8, LxA₄d4 and LtB₄d4), LC-MS/MS analysis was performed on an ultrahigh-performance liquid chromatography system (UHPLC; Agilent LC1290 Infinity) coupled to an Agilent 6460 triple quadrupole MS (Agilent Technologies) equipped with electrospray ionization operating in negative mode. Reverse-phase UHPLC was performed using a ZorBAX SB-C18 column

(Agilent Technologies) with a gradient elution. The mobile phases consisted of water, acetonitrile (ACN), and formic acid (FA) [75:25:0.1 (v/v/v)] (solution A) and ACN and FA [100:0.1 (v/v)] (solution B). The linear gradient was as follows: 0% solution B at 0 min, 85% solution B at 8.5 min, 100% solution B at 9.5 min, 100% solution B at 10.5 min, and 0% solution B at 12 min. The flow rate was 0.35 ml/min. The autosampler was set at 5°C, and the injection volume was 5 µL. Data were acquired in multiple reaction monitoring (MRM) mode with optimized conditions. Peak detection, integration, and quantitative analysis were performed with MassHunter Quantitative analysis software (Agilent Technologies). For each standard, calibration curves were built using 10 solutions at concentrations ranging from 0.95 to 500 ng/ml. A linear regression with a weight factor of 1/X was applied for each compound. The limit of detection (LOD) and the limit of quantification (LOQ) were determined for the 28 compounds using signal-to-noise (S/N) ratios. The LOD corresponded to the lowest concentration leading to an S/N value >3, and LOQ corresponded to the lowest concentration leading to an S/N value >10. All values less than the LOQ were not considered. Blank samples were evaluated, and their injection showed no interference (no peak detected), during the analysis. Hierarchical clustering was performed, and heat maps were obtained with R (www.r-project.org). PUFA metabolite amounts were transformed to z scores and clustered based on 1 – Pearson correlation coefficient as distance and the Ward algorithm as agglomeration criterion.

Microbiota analysis

DNA isolation from mouse caecal samples for sequencing

Caecal contents were collected and frozen at -80°C until use. Ten caecal contents per groups were randomly chosen between the 3 independent experiments. Metagenomic DNA was extracted from the caecal content using a QIAamp DNA Stool Mini Kit (Qiagen, Hilden, Germany) according to the manufacturer's instructions with modifications.[2]

Bacterial DNA sequencing

The bacterial 16S rRNA gene was amplified using barcoded primers V4 variable region PCR primers 515/806. After amplification, PCR products are checked in 2% agarose gel to determine the success of amplification and the relative intensity of bands. Purified PCR product is used to prepare Illumina DNA library. Sequencing was performed at MR DNA (www.mrdnalab.com, Shallowater, TX, USA) on a MiSeq (Illumina) following the manufacturer's guidelines. Sequence data were processed using MR DNA analysis pipeline (MR DNA, Shallowater, TX, USA). In brief, sequences were joined, depleted of barcodes then sequences <150bp removed, sequences with ambiguous base calls removed. Sequences were denoised, OTUs generated and chimeras removed. Operational taxonomic units (OTUs) were defined by clustering at 3% divergence (97% similarity). Final OTUs were taxonomically classified using BLASTn against a curated database derived from RDPII and NCBI (www.ncbi.nlm.nih.gov, <http://rdp.cme.msu.edu>). The analysis was completed using the Qiime2 microbiome bioinformatics pipeline (<https://qiime2.org/>).

Cell Culture

Caco2 cells (Leibniz Institute DSMZ-German Collection of Microorganisms and Cell Cultures GmbH, catalogue number: ACC 169) were cultured in DMEM medium with Glutamax (Invitrogen) supplemented with 10% heat-inactivated fetal bovine serum (Invitrogen), 1% non-essential amino acids (Fisher Scientific) and 1% antibiotics (100 U ml⁻¹ penicillin and 100 mg mL⁻¹ streptomycin; Invitrogen) at 37 °C in a 5% CO₂ atmosphere. When 70% confluence was reached, 100 000 caco2 cells were plated on Transwell inserts (Costar, Sigma Aldrich). After 15 days the measurement of paracellular permeability was performed. Dextran 4kDa-FITC (15 µM) was added on the apical side, and 24 hours after incubation, the intensity of basolateral and apical fluorescence was quantified at the excitation wavelength of 485 nm and the emission wavelength of 520 nm by a Varioskan Flash microplate reader (Fisher Scientific). The cells were considered differentiated when less than 5% dextran 4kDa-FITC was found on the

basolateral side. Once differentiated, the cells were cultivated in serum-free medium and treated or not with C18-3OH (1, 10 or 100 μ M) solubilized in 0.5% dimethylsulfoxide (DMSO; Sigma Aldrich) and then a lipid extraction of apical and basolateral supernatants and cells was carried out after 30 minutes, 2 hours, 6 hours, 12 hours and 24 hours of incubation. The compound C18-3OH was quantified in apical, basolateral side and in cells by LC-MS/MS. The effect of C18-3OH (1, 10 and 100 μ M) on paracellular permeability was quantified by the measure of dextran 4kDa-FITC flux through the monolayer of caco2 cells.

Ussing chambers

Colon and ileum biopsies or Peyer patches were mounted in Ussing chambers exposing 0.196 cm² of tissue surface to 1.5 mL of circulating oxygenated Krebs Ringer solution (NaCl 6.72g, NaHCO₃ 2.10g, 50mL of solution 1 (MgCl₂ 4.82g and CaCl₂ 3.52g qs 1L), 100 mL of solution 2 (K₂HPO₄ 4.16g and KH₂PO₄ 0.54g qs 1L) at 37°C. To study the passage through the intestinal epithelium of C18-3OH, 1 or 100 μ M of C18-3OH solubilized in Krebs Ringer was added to the luminal compartment. One hour after incubation the luminal and serosal compartments and biopsies were removed to quantify C18-3OH by LC-MS/MS. In parallel, intestinal paracellular permeability in response or not to 1 and 100 μ M of C18-3OH was assessed by measuring the mucosal-to-serosal flux of 4kDa FITC-dextran (15 μ M).

C18-3OH gavage in control mice.

Oral administration of C18-3OH (100 μ M;100 μ L) or its vehicle (PBS, 100 μ L) was performed daily during 7 days in mice. At day 7, mice were sacrificed at 30 minutes, 2 hours and 4 hours after the last gavage. Blood, ileum, Peyer patches and colon were collected in order to quantify the C18-3OH by LC-MS/MS. In a second set of experiments, mice were gavaged with C18-3OH as described above and were treated during 7 days by intraperitoneal administration of GW9662 (1 mg/kg; Interchim, Montluçon, France), an antagonist of PPAR γ , or its vehicle

(HBSS). Two hours after the last gavage, colons were harvested in order to perform real time PCR analysis of *Lfabp*, *Cxcl1*, *Fiaf* and *Cd36* (supplementary table 3).

Peroxisome proliferator-activated receptor gamma (PPAR γ) competitive ligand binding assay

The LanthaScreen time-resolved fluorescence resonance energy transfer (TR-FRET) PPAR γ competitive binding assay (Fisher scientific) was performed according to the manufacturer's protocol. Serial concentrations of rosiglitazone, C18-3OH, C16-3OH, C14-3OH, GW1929, a PPAR γ agonist or their vehicle (DMSO 2%) were incubated with GST-fused human PPAR γ -LBD, terbium-labeled anti-GST antibody, and a fluorescently labelled PPAR ligand (Pan-PPAR Green tracer) for 6 h in the dark at room temperature. The FRET signal was measured by excitation at 340 nm and emission at 520 nm for fluorescein and 495 nm for terbium. In this assay, test compounds binding to PPAR γ -LBD competed with Pan-PPAR Green tracer and replaced it, resulting in a decrease of signal. The ability to bind to the PPAR γ -LBD was measured by the decrease of the 520 nm/495 nm ratio using an EnSightTM multimode Plate Reader (PerkinElmer, Villebon-sur-Yvette, France).

Statistical analysis

Data are presented as means \pm standard error of the mean (SEM). Analyses were performed using GraphPad Prism 6.0 software (GraphPad, San Diego, CA). Comparisons between-groups were performed by Mann-Whitney test. Multiple comparisons within groups were performed by Kruskal-Wallis test, followed by Dunn's post-test or by two-way Anova followed by Bonferroni post-test. Statistical significance was accepted at $P < 0.05$. The heat map was performed with the R software (www.r-project.org).

Supplementary results: Identification of hydroxylated fatty acids produced by EcN.

In order to characterize the bacterial long chain fatty acid (LCFA) potentially implicated in probiotic properties of the probiotic strain, EcN, we performed an analysis of free fatty acid by liquid chromatography-high resolution mass spectrometry (LC-HRMS) of lipids extracted from EcN. The total ion chromatograms (TIC) obtained from the electrospray ionization (ESI) was used to reveal the lipids with the higher concentration (supplementary figure 1A). The higher peak eluted at 14.84 min correspond to the C14:3n-3 at m/z 341.27 as previously described.[3] For the peak eluted at 15.98 min, with the accurate m/z ratio 243.1959, we determined an elemental composition of the deprotonated molecule like $[(C_{14}H_{28}O_3)-H]^-$. Then, the natural isotopic profile of the molecular species in the experimental mass spectrum obtained at 15.98 min was compared to its simulation generated from the formula (calculated: m/z 243.1961). These two isotopic profiles were similar and the accuracy of the m/z measurements of monoisotopic peak was 0.8 ppm (supplementary figure 1B), as well as the m/z measurements of its first major natural isotopic $[(^{13}CC_{13}H_{28}O_3)-H]^-$ peak supporting the proposed elemental composition. Finally, MS/MS analyses were performed under HR measurement conditions by using collisional activation (supplementary figure 1C). The product ion spectrum (under normalized collision energy (NCE) = 35% conditions) showed ions at m/z 243.1959 and m/z 59.0139 that is the specific product ion from dissociation of the deprotonated carboxyl group link to a methyl. Thus, with the fragmentation pattern we identified the C14:3-OH. Consequently, the extracted ion chromatogram (EIC) of the diagnostic product ion at m/z 59.0139 corresponding to the daughter ion of a 3-hydroxyl fatty acid allowed us to identify the Cn:3-OH molecules with Cn \neq C14.

Supplementary table 1

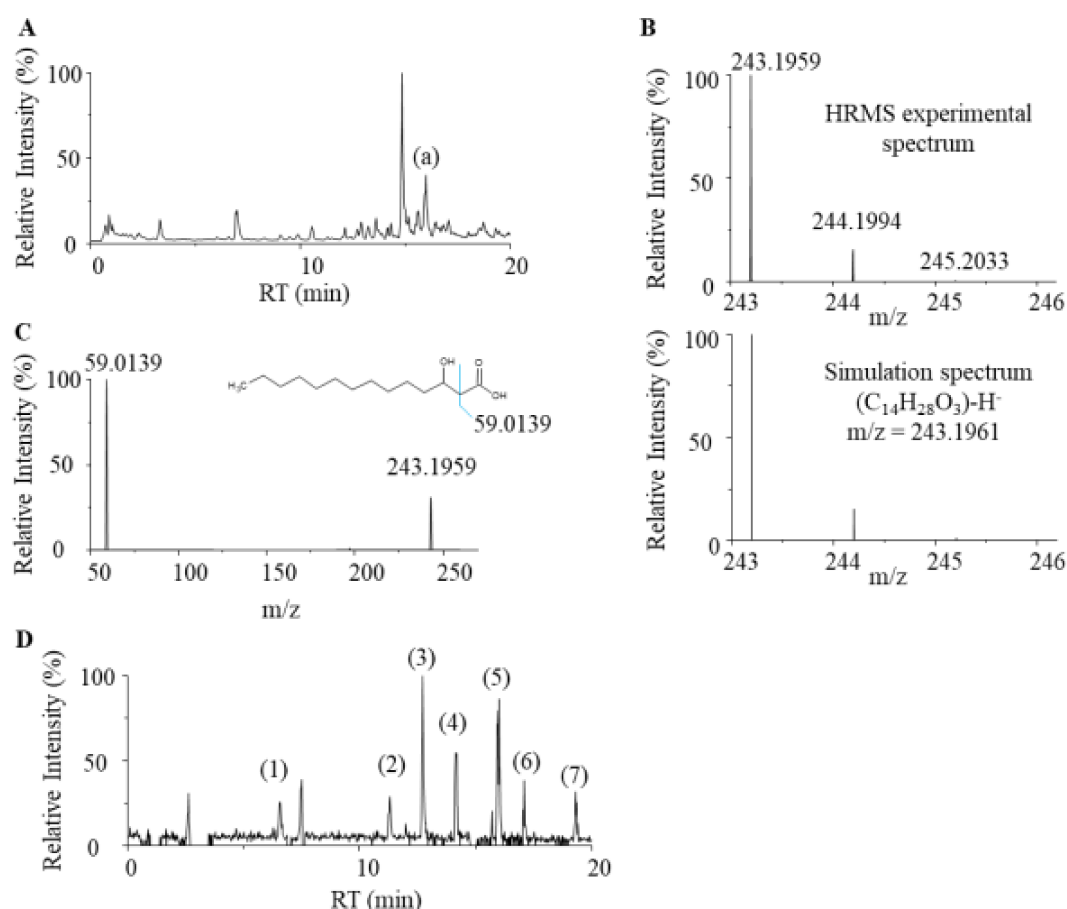
| Abbreviation | E. coli strain | | Reference |
|------------------|----------------|--------------------|--------------------------------|
| MG1655 | MG1655 | Serotype OR:K:-H48 | Blattner et al;1997 [4] |
| ECN | Nissle 1917 | Serotype O6:K5:H1 | Olier et al., 2012 [5] |
| ECN ΔcblbP | Nissle 1917 | Serotype O6:K5:H1 | Perez-Berezo T et al, 2017 [3] |
| ECN S95R | Nissle 1917 | Serotype O6:K5:H1 | Massip et al, 2019 [6] |
| ECN ΔcblbA ΔentD | Nissle 1917 | Serotype O6:K5:H1 | Massip et al, 2019 [6] |
| UTI | UTI89 | Serotype O18:K1:H7 | Mulvey et al., 2001 [7] |
| Nu14 | Nu14 | Serotype O18:K1:H7 | Johnson et al., 2001 [8] |
| SP15 | SP15 | Serotype O18:K1:H7 | Johnson et al., 2002 [9] |
| CFT | CFT073 | Serotype O6:K2:H1 | Mobley et al., 1990 [10] |
| NC101 | NC101 | Serotype O2:H6/41 | Kim et al., 2005 [11] |
| ABU | AB83972 | Serotype OR:K5:H- | Lindberg et al., 1975 [12] |
| M1/5 | M1/5 | Serotype O75:H5 | Secher et al., 2015 [13] |

Supplementary table 2

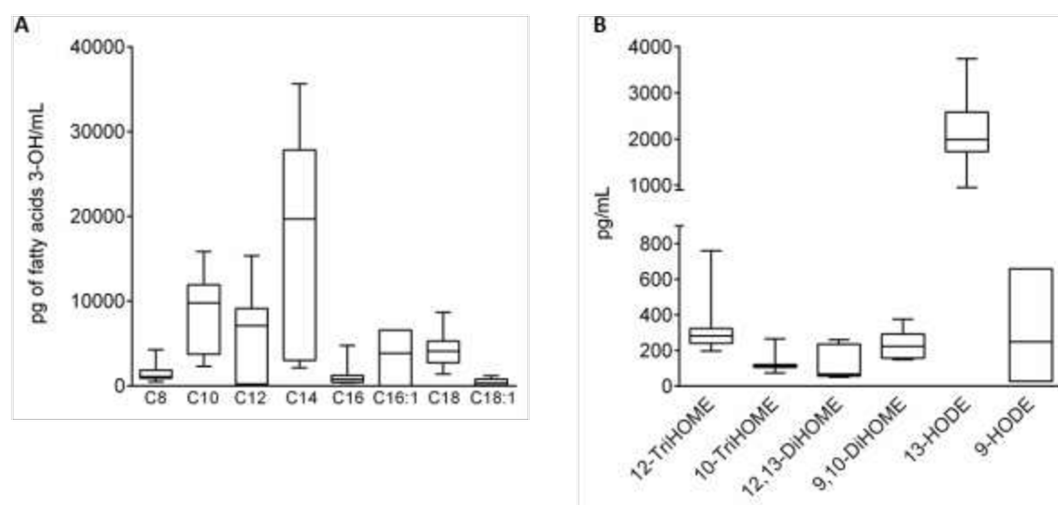
| Compound name | RT (min) | Precursor ion (m/z) | Product ion (m/z) | Fragmentor (V) | CE (V) |
|---------------|----------|---------------------|-------------------|----------------|--------|
| C8-3OH | 1.827 | 159.1 | 59.0 | 90 | 14 |
| 12-TriHOME | 3.177 | 329.2 | 211.1 | 90 | 18 |
| 10-TriHOME | 3.279 | 329.2 | 171.1 | 100 | 18 |
| C10-3OH | 4.130 | 187.1 | 59.0 | 90 | 14 |
| C12-3OH | 7.080 | 215.2 | 59.0 | 90 | 14 |
| 12,13-DiHOME | 7.184 | 313.2 | 183.1 | 85 | 18 |
| 9,10-DiHOME | 7.426 | 313.2 | 201.1 | 90 | 14 |
| 9-HOTrE | 8.707 | 293.2 | 171.1 | 80 | 10 |
| 13-HOTrE | 8.910 | 293.2 | 195.1 | 95 | 10 |
| 13-HODE | 9.969 | 295.2 | 195.0 | 135 | 8 |
| 9-HODE | 10.026 | 295.2 | 171.0 | 135 | 8 |
| C14-3OH | 10.041 | 243.2 | 59.0 | 90 | 14 |
| 13-oxoODE | 10.676 | 293.2 | 113.1 | 80 | 14 |
| 9-oxoODE | 10.946 | 293.2 | 185.0 | 100 | 14 |
| C16:1-3OH | 11.092 | 269.2 | 59.0 | 90 | 14 |
| C16-3OH | 12.952 | 271.2 | 59.0 | 90 | 14 |
| C18:1-3OH | 13.736 | 297.2 | 59.0 | 90 | 14 |
| C18-3OH | 14.243 | 299.3 | 59.0 | 90 | 14 |

Supplementary table 3

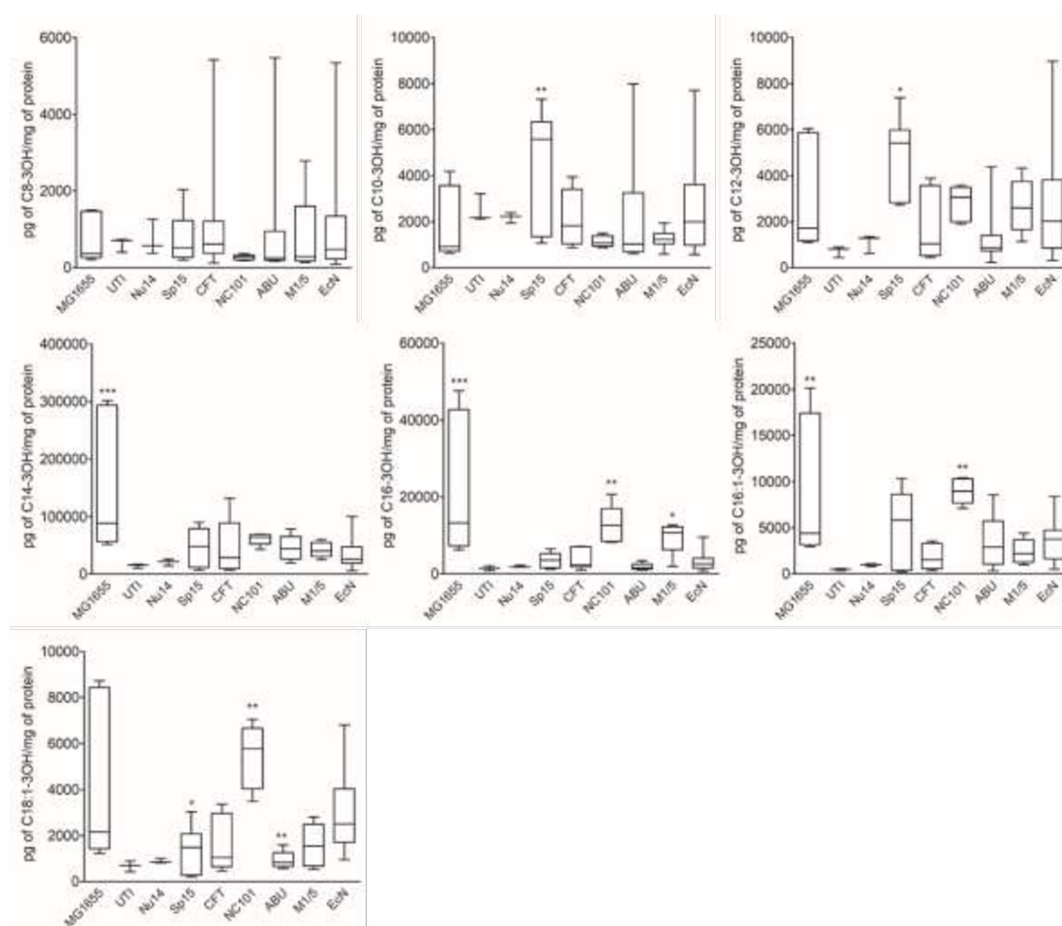
| Transcripts | Forward | Reverse |
|------------------|--------------------------|--------------------------|
| <i>Hprt</i> | GTTCTTTGCTGACCTGCTGGAT | CCCCGTTGACTGATCATTACAG |
| <i>Tff3</i> | TGCAGATTACGTTGGCCTGTC | TGGAGTCAAAGCAGCAGCC |
| <i>Muc2</i> | CGGAACTCCAGAAAGAAGCCA | GGCAGTCAGACGCAAAGTTGTA |
| <i>Occludine</i> | TGGATGACTACAGAGAGGAGAGT | TCCTCTTGATGTGCGATAATTTGC |
| <i>Tjp1</i> | AAGTTCCTGAAGCCCCTGGAG | GGAAGACACTTGTTTTGCCAGGT |
| <i>Reg3γ</i> | CCTCCATGATCAAAAGCAGTGG | GGATTTCGTCTCCCAGTTGATGT |
| <i>Mmp7</i> | ACTGATGGTGAGGACGCAGG | CATCACAGTACCGGGAACAGAA |
| <i>Tnfα</i> | CCACGCTCTTCTGTCTACTGAAC | GGTCTGGGCCATAGAACTGATG |
| <i>Ccl5</i> | ACTCCCTGCTGCTTTGCCTA | TTCCTTCGAGTGACAAACACGA |
| <i>Tgfb</i> | GACCCCCACTGATACGCCT | GCTGAATCGAAAGCCCTGTA |
| <i>Il6</i> | CTCTGCAAGAGACTTCCATCCAGT | CGTGGTTGTCAACAGCATCA |
| <i>Il1β</i> | ACCTTCCAGGATGAGGACATGAG | CATCCCATGAGTCACAGAGGATG |
| <i>Nfkb</i> | TGAAGATGTTGCTGGCCGT | GCAGATCCCTCACAAGCTGA |
| <i>Cxcl1</i> | GCTAAAAGGTGTCCCAAGTAACG | TCACCAGACAGGTGCCATCA |
| <i>Cxcl2</i> | AGCCCCCTGGTTCAGAAA | TCCAGGTCAGTTAGCCTTGCC |
| <i>Fiaf</i> | CACCCCTCAAAGACTCCGAGG | TGAGCCTTGAGCTGAGTCTGC |
| <i>Lfabp</i> | TTCAAAGGCATAAAGTCCGTGAC | GCCTTGTCTAAATTCTCTTGCTGA |
| <i>Cd36</i> | GGCCAAGCTATTGCGACATG | AAAGGTGGAAAGGAGGCTGC |



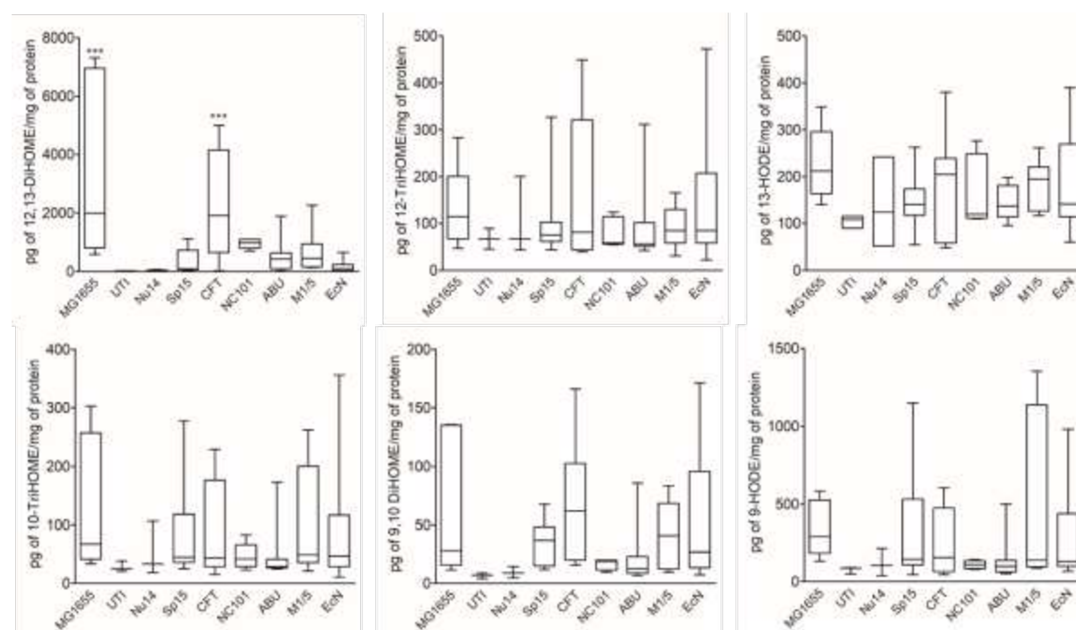
Supplementary figure 1: Identification of LCFA-3OH in bacteria by LC-HRMS. (A) Total Ion chromatogram of a lipidic extract of bacteria. (B) Natural isotopic distribution of the deprotonated molecule displayed by the high-resolution mass spectrum zoom obtained for the peak eluted at 15.98 min (a) and natural isotopic pattern calculated with the formula $[(C_{18}H_{28}O_3)-H]^-$. Analogous natural isotopic patterns and similar m/z ratios measured and simulated for the monoisotopic $[(^{12}C_{18}H_{28}^{16}O_3)-H]^-$ ion and for the $[(^{13}C_nC_{18-n}H_{28}^{16}O_3)-H]^-$ (with n = 1 and 2) ions (within an accuracy of 0.8 ppm). (C) Product ion spectrum acquired via HCD (NCE = 35%) of the carboxylate anion $[M-H]^-$ (m/z 243) generated in electrospray from the LC peak eluted at 15.98 min. (D) Extracted Ion Chromatogram (EIC) of a lipidic extract of bacteria pellet for m/z = 59.0139 corresponding to the daughter ion of a 3-hydroxyl fatty acid. Peak (1) is C10-3OH, peak (2) is C12-3OH, peak (3) is C12:1-3OH, peak (4) is C14:1-3OH, peak (5) is C14-3OH, peak (6) is C16:1-3OH and peak (7) is C16-3OH.



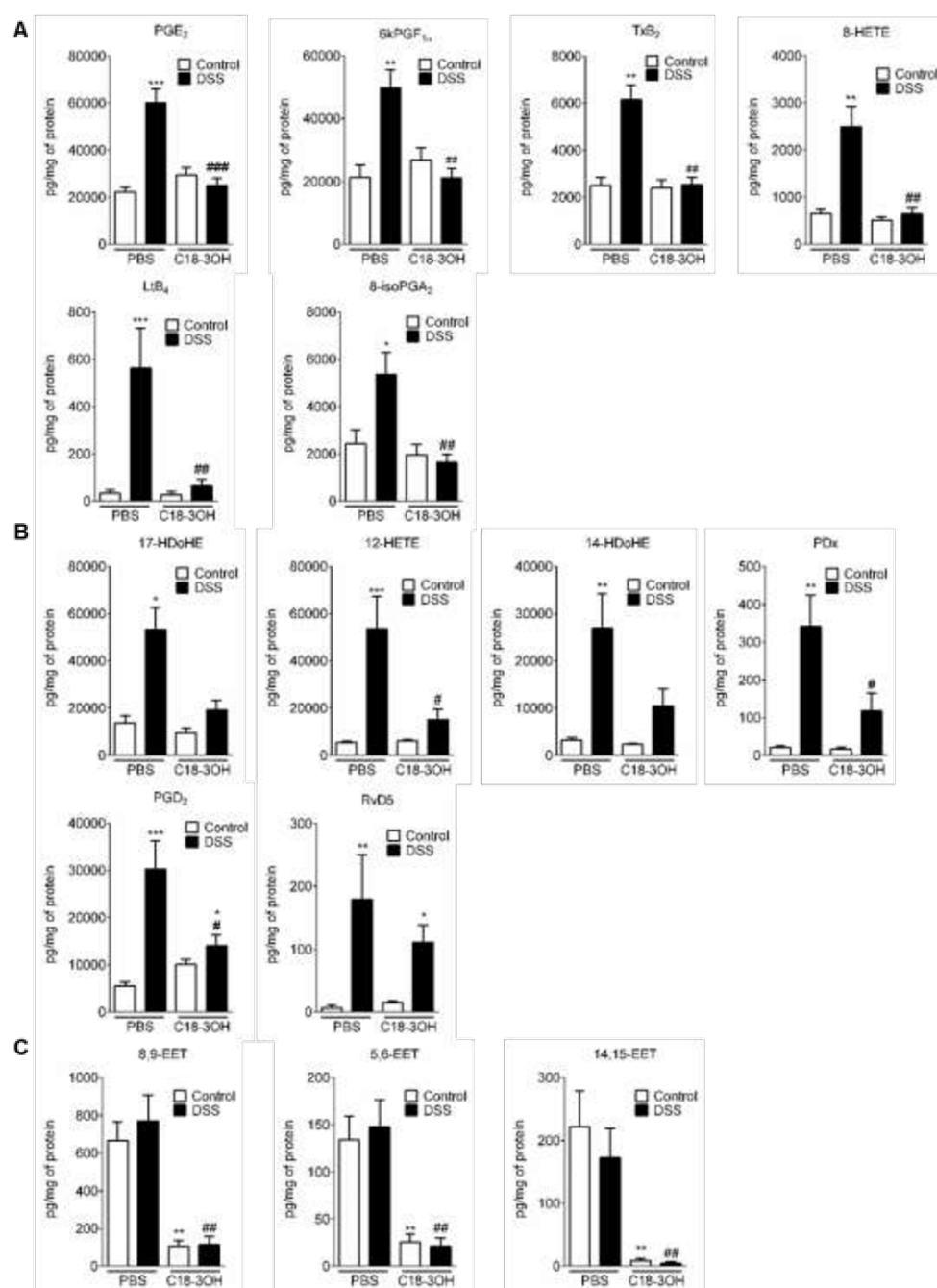
Supplementary figure 2: Quantification of hydroxylated long chain fatty acids by LC-MS/MS in EcN culture supernatant. Quantification of long chain fatty acid (LCFA) hydroxylated on the third carbon (**A**) and of metabolites from linoleic acid (C18:2 n-6) (**B**) in EcN culture supernatant. Data are represented as whiskers plot (min to max, centered value at median). N=5 to 10 experiments of three independent bacterial cultures per group.



Supplementary figure 3: Quantification of hydroxylated long chain fatty acids by LC-QQQ. Quantification of long chain fatty acid (LCFA) hydroxylated on the third carbon in pellet of the different strains of *E. coli* by LC-QQQ. Data are represented as whiskers plot (min to max, centered value at median). N=5 to 10 experiments of three independent bacterial cultures per group. Statistical analysis was performed using Kruskal–Wallis and subsequent Dunn’s post hoc test. * $p < 0.05$, ** $p < 0.01$, significantly different from EcN.

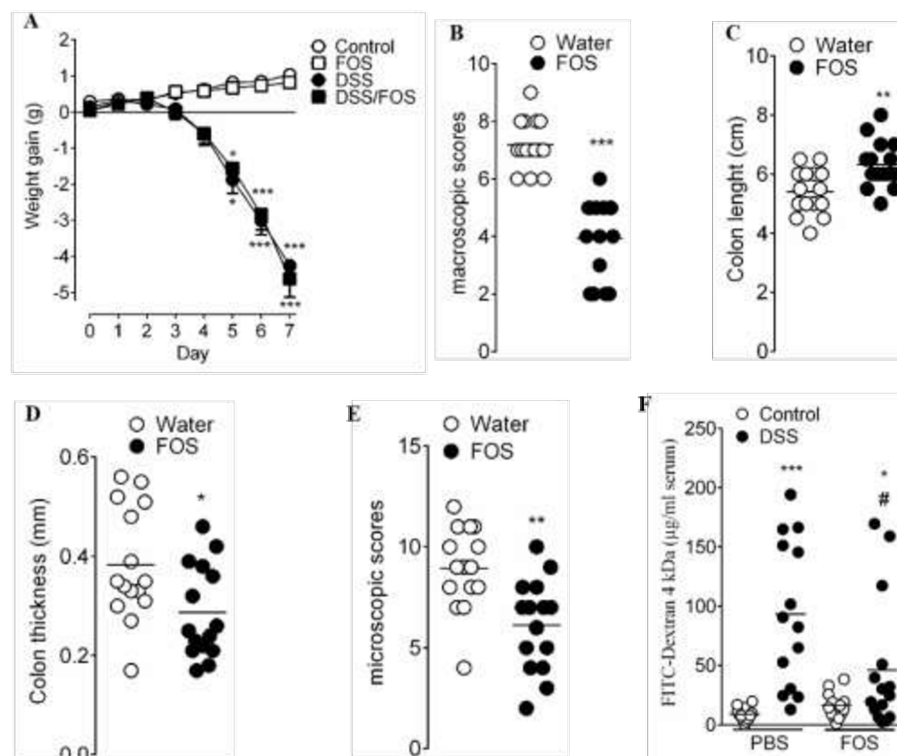


Supplementary figure 4: Quantification of hydroxylated long chain fatty acids by LC-QQQ. Quantification of linoleic acid (C18:2 n-6) metabolites in the different strains of *E. coli* by LC-QQQ. Data are represented as whiskers plot (min to max, centered value at median). N=5 to 10 experiments of three independent bacterial cultures per group. Statistical analysis was performed using Kruskal–Wallis and subsequent Dunn’s post hoc test. *** $p < 0.001$, significantly different from EcN.



Supplementary figure 5: Concentration of PUFA metabolites in mouse colon. PUFA concentration of cluster 1 (A), cluster 2 (B), cluster 3 (C) in control (white bars) and DSS-treated mice (black bars) gavaged or not with C18-3OH. Data are represented as mean ± SEM. Statistical analysis was performed using Kruskal–Wallis and subsequent Dunn’s post hoc test.

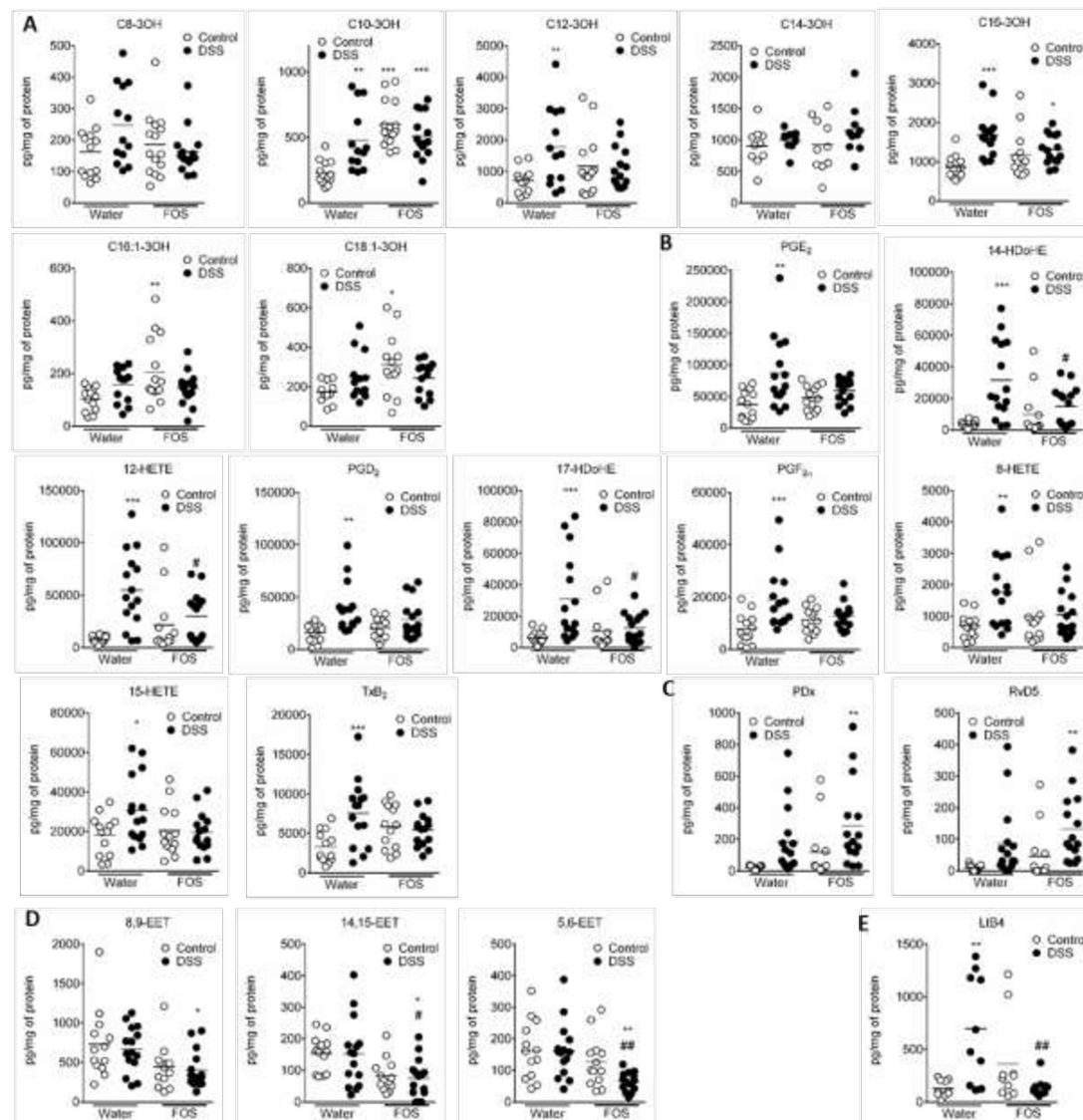
* $p < 0.05$, ** $p < 0.01$, *** $p < 0.001$, significantly different from control. # $p < 0.05$, ## $p < 0.01$,
$p < 0.001$ significantly different from DSS/PBS group.



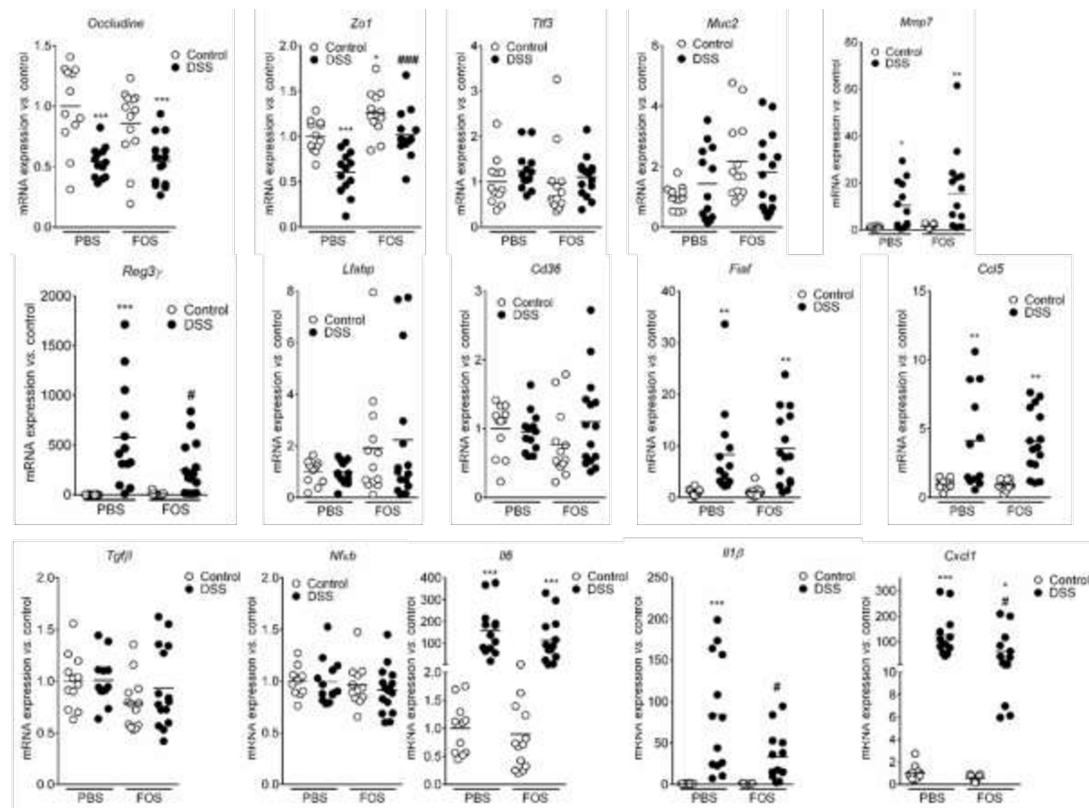
Supplementary figure 6: Fructooligosaccharides diet reduces DSS-induced colitis. (A)

Weight gain was observed in DSS-treated (black symbols) or control mice (white symbols) treated with FOS (square) or not treated (circle). Data are expressed as mean ± SEM. Statistical analysis was performed using repeated-measures 2-way ANOVA and a Bonferroni's multiple comparisons post hoc tests. * $p < 0.05$, *** $p < 0.001$ significantly different from control group. Colitis severity was assessed by macroscopic damage scores (B), colon length (C), colon thickness (D) and microscopic damage scores (E) in DSS/FOS (black symbols) or DSS (white symbols). Data are expressed as mean. Statistical analysis was performed using Mann-Whitney test. ** $p < 0.01$, *** $p < 0.001$ significantly different from water group. (F) Paracellular permeability was quantified in the serum of mice treated with the DSS (black symbols) or their control (white symbols) and treated with FOS (right symbols) or not (left symbols). Data are expressed as mean. Statistical analysis was performed using Kruskal–Wallis and subsequent

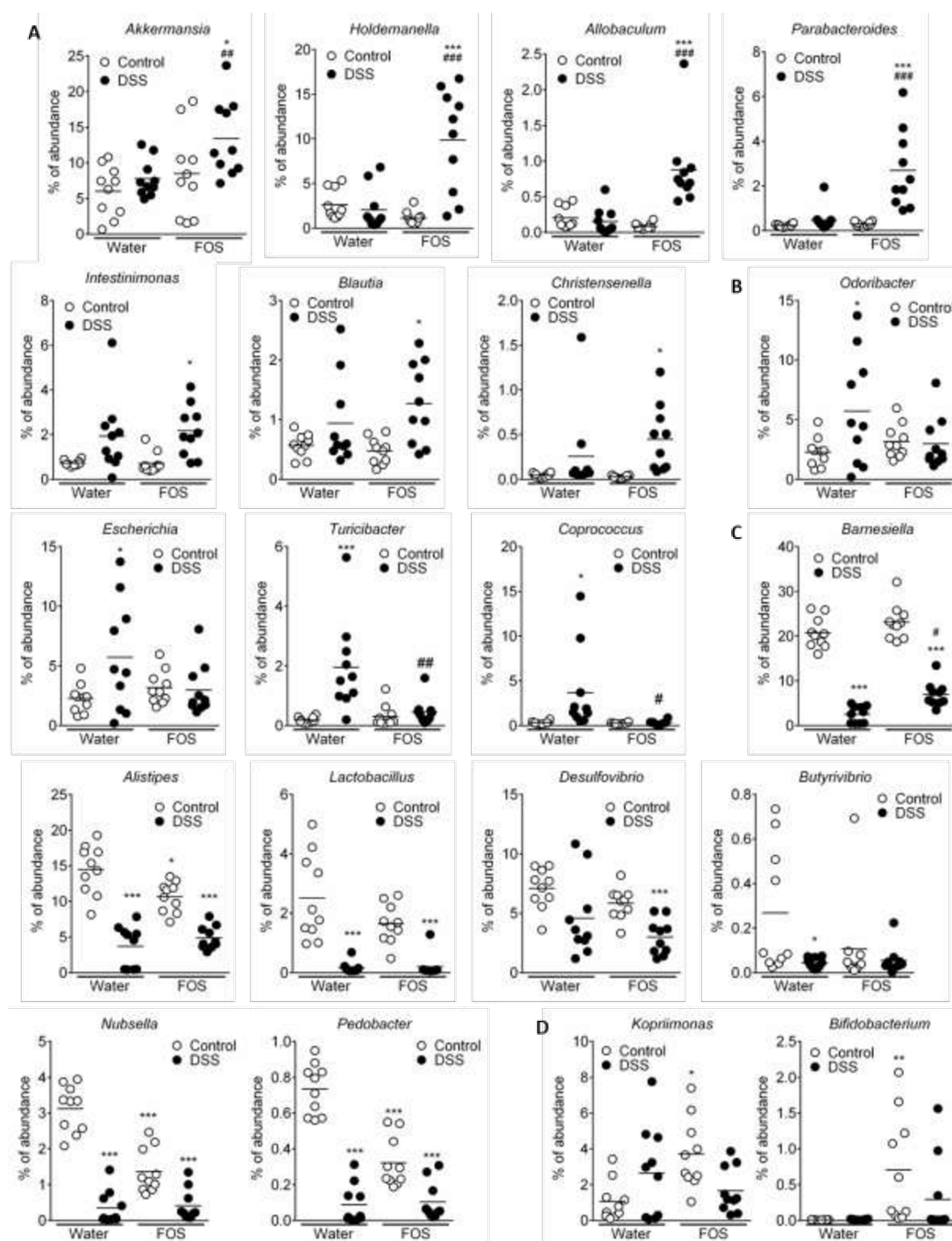
Dunn's post hoc test. * $p < 0.05$, *** $p < 0.001$, significantly different from control/PBS group and # $p < 0.05$, significantly different from DSS/PBS group.



Supplementary figure 7: Concentration of LCFA-3OH and PUFA metabolites in mouse colon. LCFA-3OH (A) and PUFA concentration of cluster 1 (B), cluster 2 (C), cluster 3 (D) and cluster 4 (E) in control (white symbols) and DSS-treated mice (black symbols) and treated or not with FOS. Data are represented as mean. Statistical analysis was performed using Kruskal–Wallis and subsequent Dunn’s post hoc test. * $p < 0.05$, ** $p < 0.01$, *** $p < 0.001$, significantly different from control. # $p < 0.05$, ## $p < 0.01$, significantly different from DSS/water group.



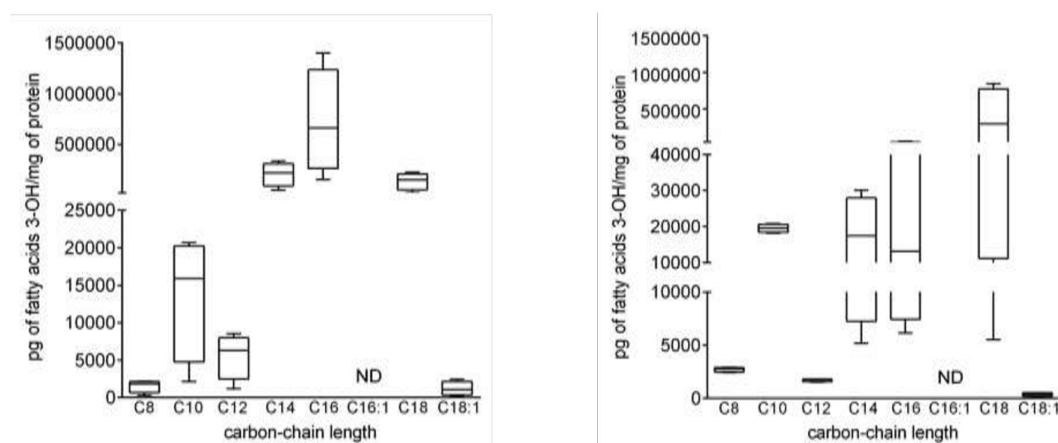
Supplementary figure 8. Fructooligosaccharides diet reduces DSS-induced pro-inflammatory genes. mRNA of several genes were quantified in colon of mice treated with the DSS (black bars) or their control (white bars) and treated with FOS (right bars) or not (water, left bars) by quantitative real-time polymerase chain reaction. mRNA content was normalized to HPRT mRNA and quantified relative to the control/PBS group. Data are expressed as mean. Statistical analysis was performed using Kruskal–Wallis and subsequent Dunn’s post hoc test. * $p<0.05$, ** $p<0.01$, *** $p<0.001$, significantly different from control/PBS group and # $p<0.05$, significantly different from DSS/PBS group.



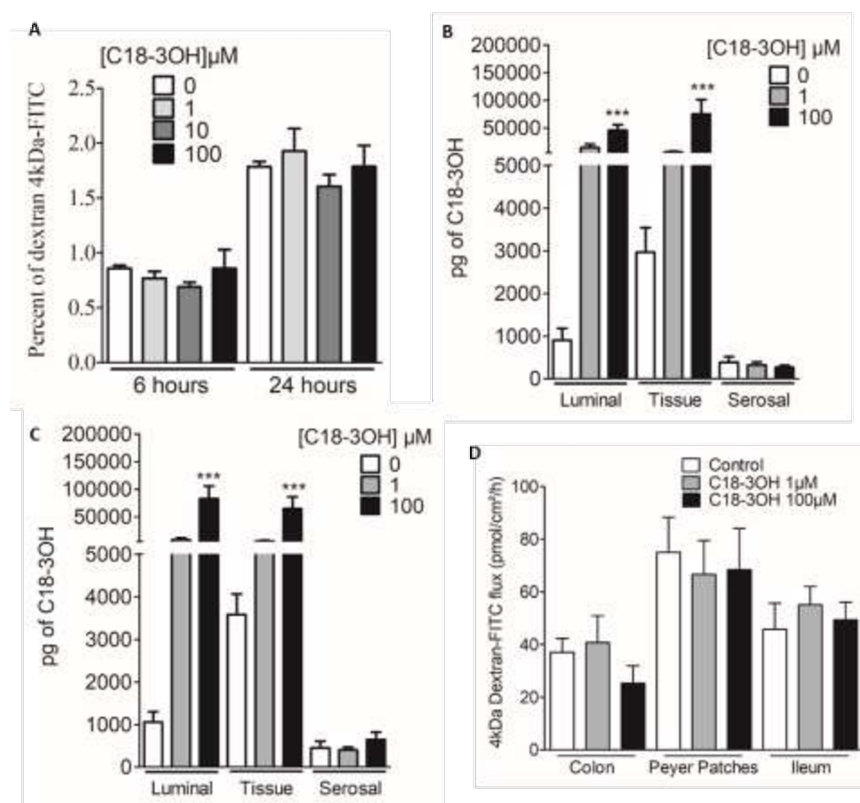
Supplementary figure 9: Percentage of abundance in genera of the first cluster.

Abundance in genera of the cluster 1 (A), 3 (B), 5 (C) and 6 (D) in the caecum of mice treated with the DSS (black symbols) or their control (white symbols) and treated with FOS (right symbols) or not (left symbols). Data are expressed as mean. Statistical analysis was performed

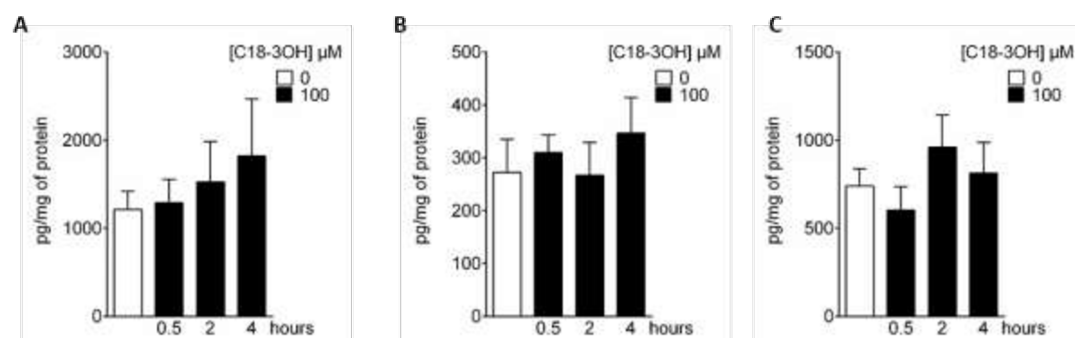
using Kruskal–Wallis and subsequent Dunn’s post hoc test. * $p < 0.05$, *** $p < 0.001$ significantly different from control/water group. # $p < 0.05$, ## $p < 0.01$, ### $p < 0.001$ significantly different from control/DSS group.



Supplementary figure 10: Quantification of hydroxylated long chain fatty acids by LC-MS/MS in *Holdemanella biformis*. Quantification of long chain fatty acid (LCFA) hydroxylated on the third carbon in pellets (left panel) and in *Holdemanella biformis* culture supernatant. Data are represented as whiskers plot (min to max, centered value at mean). N=1 experiment of four independent bacterial cultures per group.



Supplementary figure 11: C18-3OH does not cross the epithelial barrier and does not modify paracellular permeability. (A) Paracellular permeability was determined by the quantification of the FITC fluorescence in basolateral compartment of Caco2 cells cultured in Transwell 6 hours or 24 hours after the treatment by C18-3OH (0 μ M white bar, 1 μ M light gray bar, 10 μ M dark gray bar or 100 μ M black bar). One hour after treatment with C18-3OH (0 μ M white bar, 1 μ M gray bar or 100 μ M black bar) at the luminal side of an ileum biopsy (B) or Peyer's patches (C) mounted in Ussing chamber, C18-3OH was quantified in the luminal and serosal compartment and in the tissue. n=12 to 15 experiments. (D) Paracellular permeability was determined by the quantification of the FITC fluorescence in serosal compartment of Ussing chambers mounted with colon, ileum or Peyer's patches 1 hour after the treatment by C18-3OH (0 μ M white bar, 1 μ M gray bar or 100 μ M black bar). Data are represented as mean \pm SEM. Statistical analysis was performed using Kruskal–Wallis and subsequent Dunn's post hoc test. ***p<0.001, significantly different from 0 μ M of C18-3OH condition.



Supplementary figure 12: Quantification of C18-3OH along the gut and in the blood. Mice were orally treated with C18-3OH (0 μM white bar or 100 μM black bar) every day during 7 days and C18-3OH was quantified 30 minutes, 2 hours and 4 hours after the last gavage in the ileum (**A**), the Peyer's patches (**B**) and the blood (**C**). Data are represented as mean \pm SEM. Statistical analysis was performed using Kruskal–Wallis and subsequent Dunn's post hoc test.

Supplementary references

- 1 Le Faouder P, Baillif V, Spreadbury I, *et al.* LC-MS/MS method for rapid and concomitant quantification of pro-inflammatory and pro-resolving polyunsaturated fatty acid metabolites. *J Chromatogr B Analyt Technol Biomed Life Sci* 2013;**932**:123-33.
- 2 Everard A, Lazarevic V, Gaia N, *et al.* Microbiome of prebiotic-treated mice reveals novel targets involved in host response during obesity. *ISME J* 2014;**8**:2116-30.
- 3 Perez-Berezo T, Pujo J, Martin P, *et al.* Identification of an analgesic lipopeptide produced by the probiotic *Escherichia coli* strain Nissle 1917. *Nat Commun* 2017;**8**:1314.
- 4 Blattner FR, Plunkett G, 3rd, Bloch CA, *et al.* The complete genome sequence of *Escherichia coli* K-12. *Science* 1997;**277**:1453-62.
- 5 Olier M, Marcq I, Salvador-Cartier C, *et al.* Genotoxicity of *Escherichia coli* Nissle 1917 strain cannot be dissociated from its probiotic activity. *Gut Microbes* 2012;**3**:501-9.
- 6 Massip C, Branchu P, Bossuet-Greif N, *et al.* Deciphering the interplay between the genotoxic and probiotic activities of *Escherichia coli* Nissle 1917. *PLoS Pathog* 2019;**15**:e1008029.
- 7 Mulvey MA, Schilling JD, Hultgren SJ. Establishment of a persistent *Escherichia coli* reservoir during the acute phase of a bladder infection. *Infect Immun* 2001;**69**:4572-9.
- 8 Johnson JR, Weissman SJ, Stell AL, *et al.* Clonal and pathotypic analysis of archetypal *Escherichia coli* cystitis isolate NU14. *J Infect Dis* 2001;**184**:1556-65.
- 9 Johnson JR, Oswald E, O'Bryan TT, *et al.* Phylogenetic distribution of virulence-associated genes among *Escherichia coli* isolates associated with neonatal bacterial meningitis in the Netherlands. *J Infect Dis* 2002;**185**:774-84.
- 10 Mobley HL, Green DM, Trifillis AL, *et al.* Pyelonephritogenic *Escherichia coli* and killing of cultured human renal proximal tubular epithelial cells: role of hemolysin in some strains. *Infect Immun* 1990;**58**:1281-9.
- 11 Kim SC, Tonkonogy SL, Albright CA, *et al.* Variable phenotypes of enterocolitis in interleukin 10-deficient mice monoassociated with two different commensal bacteria. *Gastroenterology* 2005;**128**:891-906.
- 12 Lindberg U, Claesson I, Hanson LA, *et al.* Asymptomatic bacteriuria in schoolgirls. I. Clinical and laboratory findings. *Acta paediatrica Scandinavica* 1975;**64**:425-31.
- 13 Secher T, Payros D, Brehin C, *et al.* Oral tolerance failure upon neonatal gut colonization with *Escherichia coli* producing the genotoxin colibactin. *Infect Immun* 2015;**83**:2420-9.